

GPS Receiver Autonomous Interference Detection

Awele Ndili, *Stanford University*
Dr. Per Enge, *Stanford University*

Presented at the 1998 IEEE Position, Location and Navigation Symposium - PLANS '98
Palm Springs, California
April 1998

ABSTRACT

Interference presents a challenge in the use of GPS for aircraft high precision approach, by posing a threat to the accuracy and integrity of the GPS navigation solution. Such interference may result from 'unintentional' sources (such as TV/FM harmonics, Radar, MSS), or may result from hostile (jamming) efforts.

This research focuses on algorithms for on-board interference detection and monitoring. Types of interference considered include coherent CW and broadband, pulsed and continuous. We study the effects of different types of interference on GPS receiver measurements. From simulation and bench test validation we present interference detection algorithms based on the observable effects of the various types of interference on the GPS receiver derived measurements.

Interference detection is based on a combination of the following test statistic - correlator output power, variance of correlator output power, carrier phase vacillation, and AGC control loop gain. The role and benefits of pseudolites in reducing the adverse effects of interference are also discussed.

1. INTRODUCTION

Integrity can be defined as a measure of confidence on the specified accuracy of any given system. Precision GPS applications such as CAT II/III aircraft landings place demands for high levels of integrity from a GPS receiver, given the risks involved. Unfortunately RF interference, which occurs frequently in the operating environment of a GPS receiver, can surreptitiously degrade accuracy, and thereby compromise the integrity of the receiver. Such interference may be intentional (from an RF jammer) or non-intentional, as would result from channel cohabitation or harmonics from mobile cellular, satellite, TV and FM radio. Figure 1 below shows the degradation in pseudorange accuracy of a receiver subjected to CW and AWGN interference¹.

¹ Results are from software simulation described in following sections.

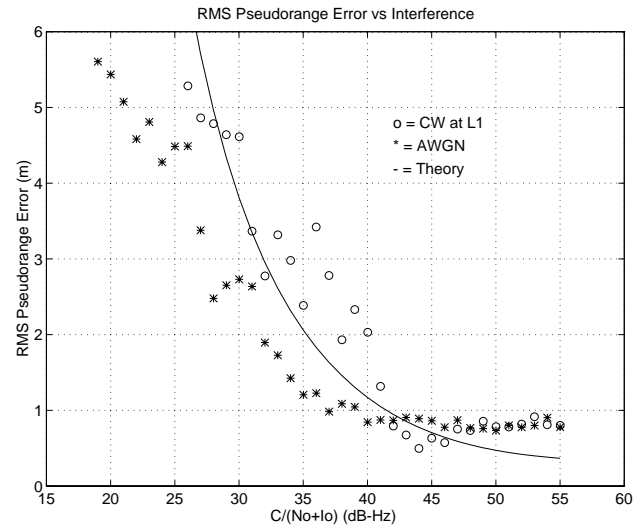


Figure 1: Pseudorange Error vs. $C/(N_o+I_o)$ for AWGN and CW Interference

The figure shows an increase in pseudorange error from a nominal level of 0.8 meters to over 5 meters with increasing interference, or equivalently, decreasing C/N_o . In normal GPS operation, this degradation in accuracy is unobservable. Thus applications having stringent accuracy requirements would experience a compromise in integrity. The main thrust of this research is to minimize this integrity risk by reliable early detection of the presence of RF interference.

Previous approaches to GPS integrity monitoring include ground-based methods [1]. While being a necessary measure, ground based monitoring is not sufficient however, since in certain scenarios, interference to on-board receivers may be unobservable from a ground-based monitor. It is therefore important to have an independent on-board integrity monitor. Other approaches have focused on monitoring measurement residuals, computed at the navigation filter of the receiver [7].

This research presents methods to boost the intrinsic integrity of a receiver by studying the fundamental effects of various types of interference on low-level or raw receiver measurements. Receiver measurements

investigated include correlator output power, variance of correlator output power, carrier phase vacillation, and adaptive analog-to-digital converter thresholds, defined in section 2. The first three measurements are derived from the basic inphase/quadrature measurements of a receiver. Types of interference studied include AWGN, coherent CW at different frequencies, pulsed interference, and signal attenuation as may result from multipath or satellite blockage. Tools used for analyses include software simulation and bench test validation, described in section 2. Based on results of this study, presented in section 3, we demonstrate the effectiveness of these candidate parameters as decision statistics for integrity monitoring.

2. SIMULATION AND BENCH TEST SETUP

2.1 Simulation Setup

A GPS constellation and receiver software simulation was developed as a tool to study the effects of interference on raw receiver measurements. An open architecture model was adopted, making it possible to simulate specific receiver types by varying input configuration files.

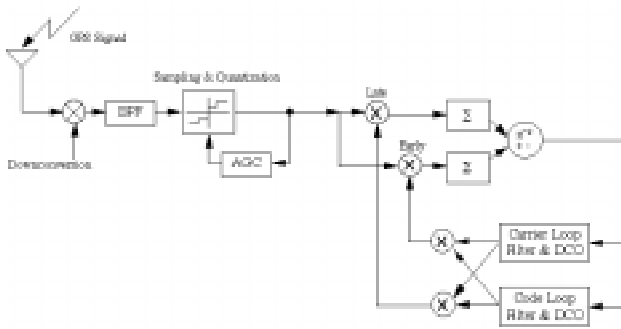


Figure 2: Schematic of Computer Simulation

Figure 2 shows a schematic of the software simulation, which is described under subsequent subsections:

2.1.1 Signal Generation:

The composite RF GPS signal is generated for all satellites in view for a user located at San Francisco International airport (SFO), based on an almanac downloaded from a real GPS receiver. Weightings are applied as a function of satellite elevation to account for attenuation of signal power of low elevation satellites. This weighting was derived from a curve fit to data observed over a period of time from a GPS receiver located Stanford University. Doppler effects are also taken into account for all simulated satellites.

2.1.2 Down Conversion:

The RF signal is down-converted via a three stage process to an intermediate frequency of 4.31 MHz. Interference is then added to this analog IF signal, which is then passed

through a band-pass filter with a 2 MHz pass band. Output from the filter is sampled and quantized.

2.1.3 Digitization:

Digitization consists of down-conversion by sampling at a frequency of 5.71 MHz, followed by quantization. The adaptive 2-bit analog-to-digital quantizer performs the task of an active gain control (AGC) by varying quantizer thresholds to ensure specific ratios of the output digitized quantities are maintained. Feedback from the quantizer output drives the AGC control.

2.1.4 Correlation:

The final stage in the RF to baseband conversion process consists of correlation with generated early and late inphase and quadrature signals. The correlator output signals, at baseband, are then summed in an integrate-and-dump with an integration time of 1ms. Output from the correlators drive the code and carrier loops. Early and late channels are spaced a quarter chip from prompt.

2.1.5 Code and Carrier Tracking:

Early and late correlation channels are combined to form a virtual prompt channel, which feeds the carrier tracking loop. A frequency locked loop (FLL) is used for carrier tracking, offering better performance with interference than conventional phase locked loops [4]. Code tracking employs a second order delay lock loop.

2.2 Interference Models

Noise models were developed to generate the following kinds of interference:

- AWGN:
 - bandpass filtered to 2 MHz bandwidth;
 - NSR varied from 0 dB to loss of lock;
- Coherent CW:
 - dead-on the 0th, 1st and 7th spectral lines²
 - ISR varied from 0 dB to loss of lock;
- Pulsed broadband:
 - peak AWGN interference power = + 30 dBm;
 - duty cycle varied from 0% to loss of lock;
- Pulsed CW:
 - peak CW interference power = + 30 dBm;
 - duty cycle varied from 0% to loss of lock;
- Signal Attenuation:
 - the effect of signal attenuation that may result from multipath, signal blockage or fading.
 - selected satellite signal is attenuated from nominal to loss of lock.

² The 1st and 7th spectral lines were chosen as normal and worst case interference scenarios, respectively.

2.3 Candidate Integrity Monitor Decision Statistics

Description of all four candidate test statistics follows. Note that since the first three quantities (correlator output power, its variance, and carrier phase vacillation) are derived from inphase / quadrature correlator measurements, they are channel or satellite specific. The AGC gain varies with overall SNR, and is therefore not channel specific.

2.3.1 Correlator Output Power

The correlator output power (COP) is a quantity computed in the receiver which gives an indication of the average post-correlation signal to noise ratio. It is computed from equation 1 below:

$$\text{Correlator Output Power} = \frac{I^2 + Q^2}{\text{Expected Noise Floor}} \quad (1)$$

where I and Q are the 1ms-averaged in-phase and quadrature prompt correlator signal. Expected noise floor is receiver specific, and is derived from statistic expectations for a specific receiver digital implementation. For the results discussed below, the correlator output power shown is averaged over 1 second immediately after introduction of interference.

2.3.2 Correlator Output Power Variance

Correlator Output Power Variance (COP- σ) is defined as the variance of the COP. Figure 3 shows COP for a single channel of a real receiver (GEC Plessey GPS card) immediately before and after acquisition of satellite PRN 17. The figure shows a step increase in COP and a reduction in COP- σ immediately following signal

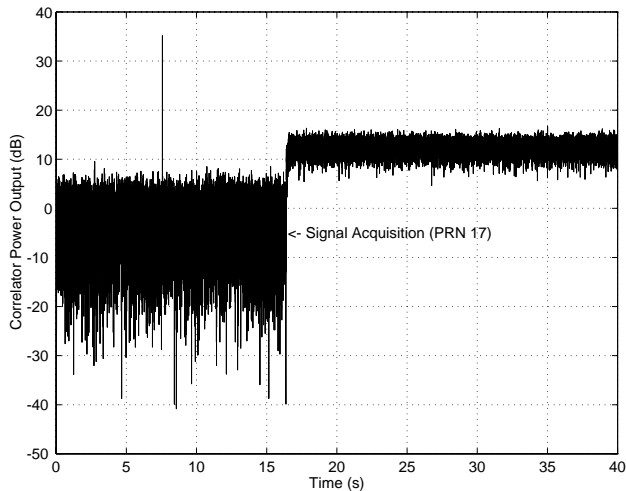


Figure 3: Correlator Output Power for a GPS Receiver

acquisition. We observe that the level and variance of COP are functions of noise in the signal, and therefore are suitable candidates for integrity monitor statistics. For the results discussed below, the COP- σ shown is averaged

over 1 second immediately after introduction of interference.

2.3.3 Carrier Phase Vacillation

Carrier phase vacillation provides a measure of the variance or jitter in carrier phase measurements from one measurement epoch to the next, and is defined here as:

$$\text{Carrier Phase Vacillation} = \text{time average}[\text{abs}\{\text{Carrier Phase}_i - \text{Carrier Phase}_{i-1}\}]$$

where i is the 1 ms epoch index. The carrier phase referenced above is computed from the arctangent of inphase and quadrature phase measurements. Averaging is performed over 1 second immediately following the introduction of interference. Large ($\pm 180^\circ$) phase swings such as may result from data bit changes, are taken into account and do not affect the computed time average. Carrier phase vacillation results are presented in degrees.

Figure 4 shows the carrier phase of a real GPS receiver tracking satellite PRN 17. The receiver incorporates a FLL carrier tracking loop. The figure shows data over a half second period and thus captures the 180 degree flips in the I/Q phasor for 50 Hz data bit changes. Carrier phase vacillation computed for this case is 11 degrees. We observe that this quantity is a function of the noise present in the signal, and therefore a candidate integrity statistic.

Note that receiver clock noise as well as interference contribute to vacillations in carrier phase measurement. This study however focuses only on the contribution of interference.

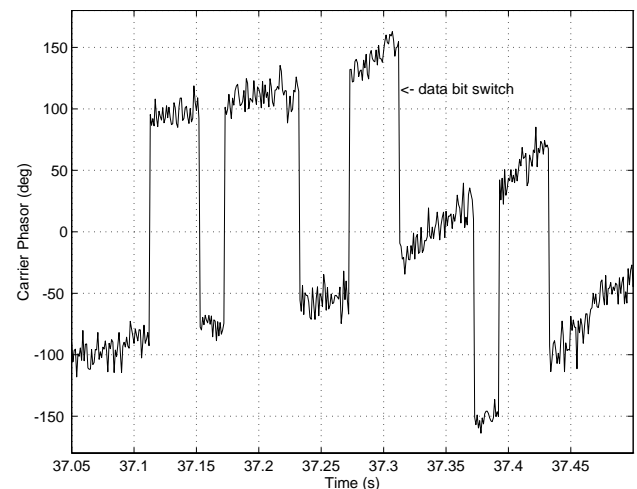


Figure 4: Carrier Phase for a GPS Receiver with a FLL Carrier Tracking Loop

2.3.4 AGC Gain

The control loop of the active gain controller (AGC), located on the signal down-conversion/digitization path, acts by adjusting the threshold levels (r_1 , r_2 and r_3 in

figure 5 below) of the 2-bit adaptive analog-to-digital converter to maintain a specified ratio of digitized signal output levels. In this application, the quantizer threshold level is therefore synonymous with AGC gain and is the quantity shown in the results.

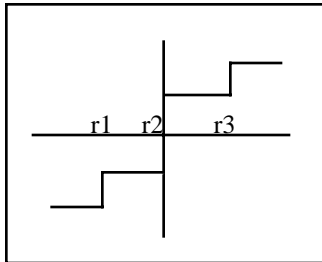


Figure 5: 2-Bit Quantizer Thresholds (AGC gain)

For an RF signal $r2=0$, and usually $r3=-r1$. Included results show averaged values of $r3$.

2.4 Test Procedures

For each run the receiver-under-test (RUT) was first allowed to acquire the GPS signal and attain steady state tracking mode in the absence of interference. The RUT was then subjected to a fixed level of each specified type of interference. The specified level is increased on subsequent runs until the loss-of-lock threshold is exceeded, causing the receiver to go into coast-mode. True pseudorange error, as measured by code tracking loop error, was recorded on each run, as well as the 1-ms time averaged values for correlator output power, COP- σ , carrier phase vacillation and AGC gain. Results are presented only for the interference regime prior to the onset of coasting, since the coast-mode can be made to trigger an alarm, thereby preserving integrity.

For the pulsed interference tests, a random pulsing scheme was adopted. Peak pulse power equivalent to +30 dBm was maintained, and pulse duty cycle varied to achieve varied loading.

It was necessary in all simulation runs to add some nominal level of 'background' AWGN to the input signal corresponding to the expected receiver thermal noise floor, in order to keep the tracking loops operational.

2.5 Bench Test Validation

Validation of the software was performed using a real GPS receiver. The receiver-under-test was a GEC Plessey GPS receiver, with a similar configuration to the simulated receiver. CW interference was generated using a Hewlett Packard HP8648B signal generator. Broadband noise was obtained from a custom Welnavigate broadband noise

generator. The bench test setup is shown below in figure 6. Bench test procedures were similar to simulation. Results were compared to software predictions to validate simulation results.

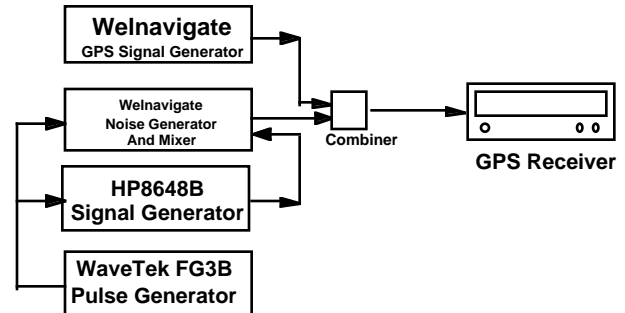


Figure 6: Bench Test Setup

3. RESULTS

3.1 Integrity Monitoring Overview

The objective of integrity monitoring is to reliably detect normally unobservable but detrimental effects of interference, in our case increasing pseudorange error, from observation of our chosen test statistics. A good decision statistic should therefore correlate closely with increasing levels of interference and deteriorating pseudorange accuracy. In addition the decision statistic should be insensitive to variations in *types* of interference in order to be robust. An ideal test statistic, therefore, when plotted against real pseudorange error, would follow the general trend indicated as 'desirable' in figure 7 below, for all types of interference. It is undesirable to have a stray set of points fall into the missed detection zone, as this constitutes a direct integrity threat. However it is tolerable to have few points fall in the false alarm region, for rare occurrences, as this is not an integrity threat but a continuity nuisance.

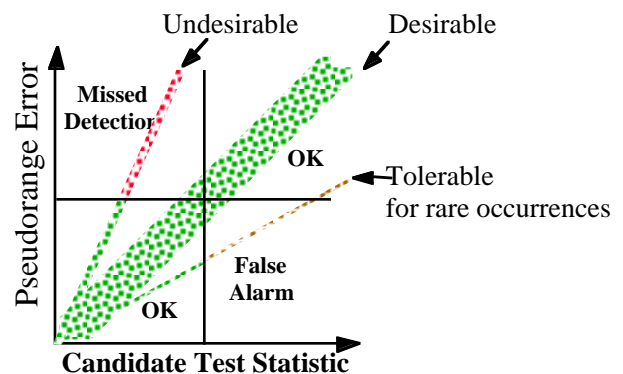


Figure 7: Test statistic characteristics

Robustness is a real issue in practice as test statistic tend to respond differently to various kinds of interference. A sample case is shown in figure 8 which shows the simulation results of comparing the effect of AWGN and CW interference on correlator output power. The figure

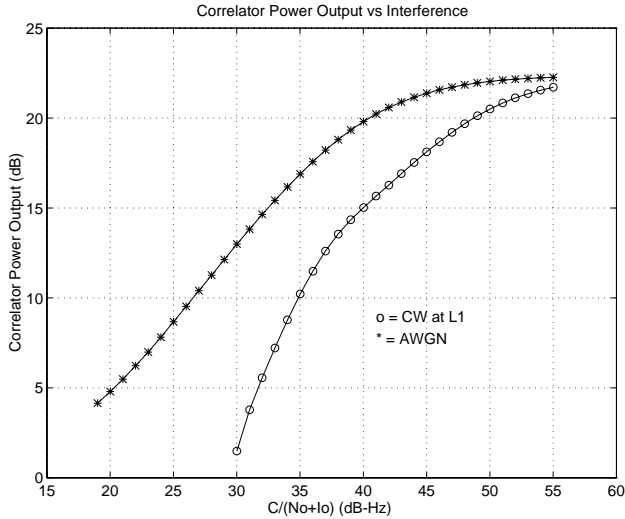


Figure 8: Correlator Output Power vs. $C/(N_o+I_o)$ for AWGN and CW Interference

shows that for the same level of input interference power, different correlator output power values result for CW vs. AWGN, with CW producing more severe COP degradation as we would expect from spread spectrum theory. However the key issue of concern is how robust the test statistics are in detecting the underlying degradation in pseudorange accuracy, as caused by the interference.

3.2 Test Statistic Results

To enable the loose definition of regions of normal operation, missed detection, false alarm and normal detection, a pseudorange error protection limit of 2 meters was chosen (horizontal line). The decision statistic threshold (vertical line) was then chosen such that there was zero incidence of missed detection for the runs with AWGN and CW interference with 0 Hz doppler offset. Note that this choice of statistic threshold level is by no means optimized, and is only used here to provide a measure of the effectiveness of each candidate decision statistic. Also note that a real statistic may include margins around the transition boundaries to account for border-line interference and pseudorange error situations, which are present in our simulation since interference is gradually increased from nominal to severe. The result in our case is that our definition of a false alarm region is extremely conservative, and produces a higher false alarm count than would occur with optimized thresholds.

Table 1 summarizes all runs, shown in figures 9 through 12. As indicated in table 1 these figures show the

observable quantities in use as decision statistic to detect degradation in pseudorange accuracy when the GPS receiver is subjected all seven forms of interference. Note that figure 9 has a reversed x-axis when compared with the schematic in figure 7.

Causes	Effects	
	Unobservable	Observable
1. AWGN	y-axis Pseudorange accuracy degradation	x-axis COP COP σ Carrier phase vacillation AGC Gain
2. CW at 0Hz offset		
3. Pulsed AWGN		
4. Pulsed CW		
5. CW at 1kHz offset		
6. CW at 7kHz offset		
7. Signal Attenuation		

Table 1: Summary of Runs

Figure 9 shows a linear correlation between pseudorange error and correlator output power for all types of 7 types of interference considered. With zero missed detection, most points lie in the regions of normal operation and normal detection, with the exception of the stray points from coherent CW at 7 kHz offset - worst case spectral line. This form of interference, precise CW jamming, is most severe, and also very difficult to sustain in practice, as the jammer would need to maintain accurate knowledge of both satellite doppler frequency shifts and platform dynamics to stay on a specific spectral line for any reasonable length of time. It is therefore a rare occurrence. Integrity is not compromised, but continuity is.

Note also in figure 9, as the intensity of CW interference on the severe 7 kHz spectral line increases, loop capture occurs as the curve doubles back on itself. Therefore integrity monitoring via correlator output power would have to also monitor CRC or data integrity to detect loop captures.

Figure 10 shows COP σ as a test statistic to detect pseudorange error degradation from interference. A similar relationship is observable as with COP. While COP σ does not show as narrow a cluster around a linear fit as COP in figure 9, it does show robustness even in the case of coherent CW jamming on the worst case spectral line.

Carrier phase vacillation in figure 11 shows a similar result to COP σ with results being much more sensitive to threshold selection than any of the other test statistics. This statistic presents larger false alarm cross-section. No special sensitivity to severe coherent CW is indicated.

Figure 12 shows AGC gain used as a detector for pseudorange error. With 4 of the 7 types of interference

(AWGN, CW at 0, 1 and 7 kHz doppler offsets), AGC follows a similar trend as the previous test statistic, showing an approximately linear correlation with pseudorange error. However markedly different results occur for pulsed interference and signal attenuation. Figure 12 shows a greatly increased sensitivity of AGC gain with pulsed interference as indicated by the almost horizontal slope of lines for pulsed AWGN and CW interference. This occurs due to the action of the multibit adaptive quantizer as it tries to suppress the pulses. The level of pulse suppression is a function of the time constant on the active gain controller.

In the case of signal attenuation, AGC gain shows little or no sensitivity at all, as indicated by the almost vertical line in figure 12. This property also is to be expected, since AGC is sensitive the total power in the incoming.

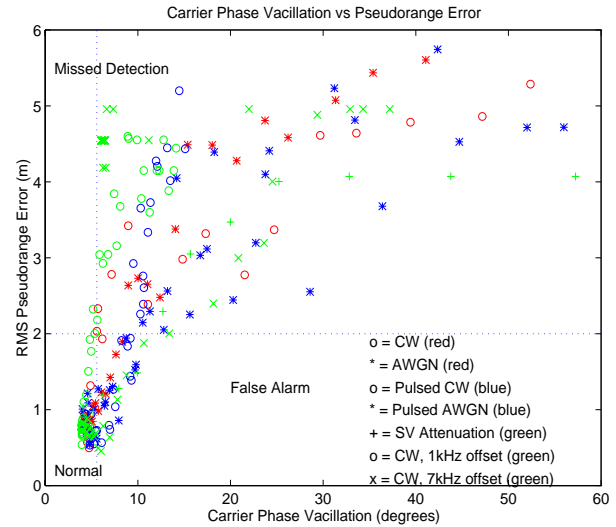


Figure 11: Pseudorange Error vs. Carrier Phase Vacillation.

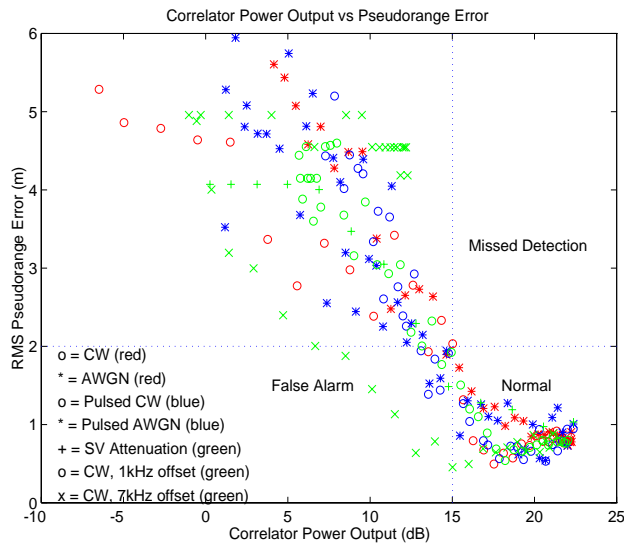


Figure 9: Pseudorange Error vs. Correlator Output Power

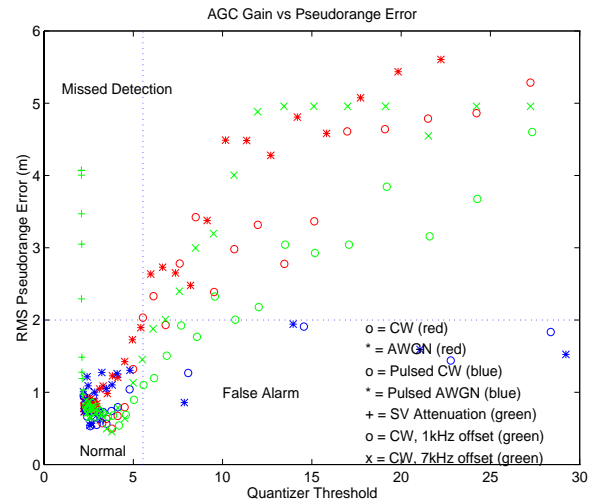


Figure 12: Pseudorange Error vs. AGC Gain

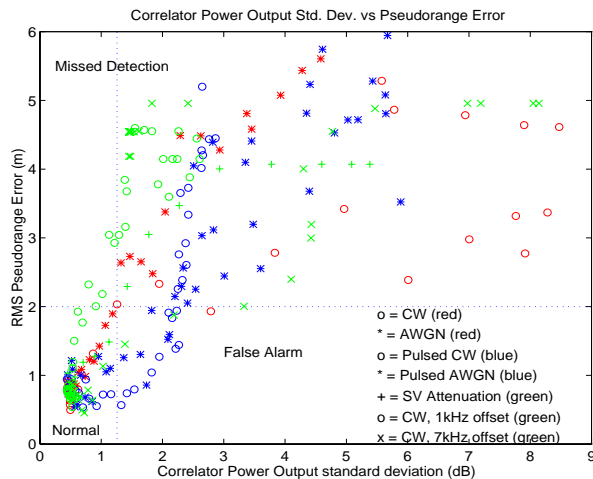


Figure 10: Pseudorange Error vs. Correlator Output Power Variance.

signal, which includes signals from all satellites in view, and receiver thermal noise. Therefore the attenuation of a single satellite signal would not significantly affect AGC gain

This peculiarity of AGC gain can be used in conjunction with other the test statistics to discriminate between pseudorange accuracy degradation due to pulsed and non-pulsed interference, and signal blockage.

3.3 Bench Test Validation Results

With a real GPS receiver, access to true pseudorange error is not readily available. We therefore compare similar observable and accessible quantities from bench test and simulation to gain confidence in our simulation. Access to AGC gain required manufacturer hardware modification, and was therefore omitted.

Figures 13, 14 and 15 show correlator output power, $COP\sigma$ and carrier phase vacillation plotted against C/N_0 for AWGN interference, with bench test results superimposed over simulation results for same type receiver with similar noise floors. A series of 14 bench test runs are shown superimposed over a single simulation run, shown as the continuous line interspersed with '*'. As seen from the figures there is a close match between bench test results and the software model, within 1 dB for both COP and $COP\sigma$ over the entire range from mild to severe interference, and within 5 degrees for carrier phase vacillation over the range 10 to 45 degrees. This close agreement lends confidence to our software model.

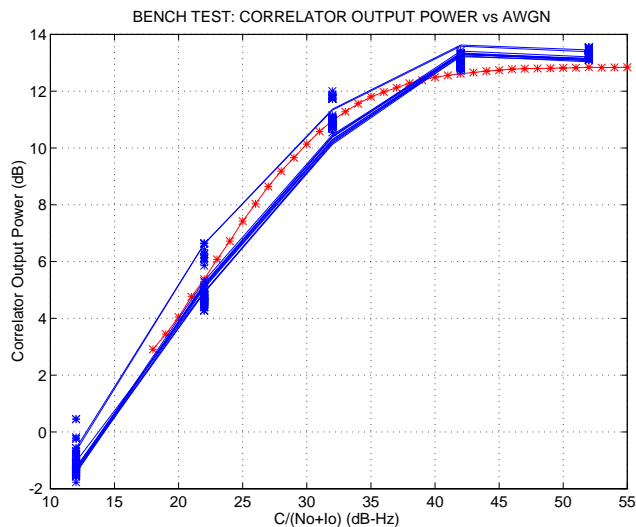


Figure 13: Correlator Output Power vs C/N_0 , AWGN, for Bench Test and Simulation.

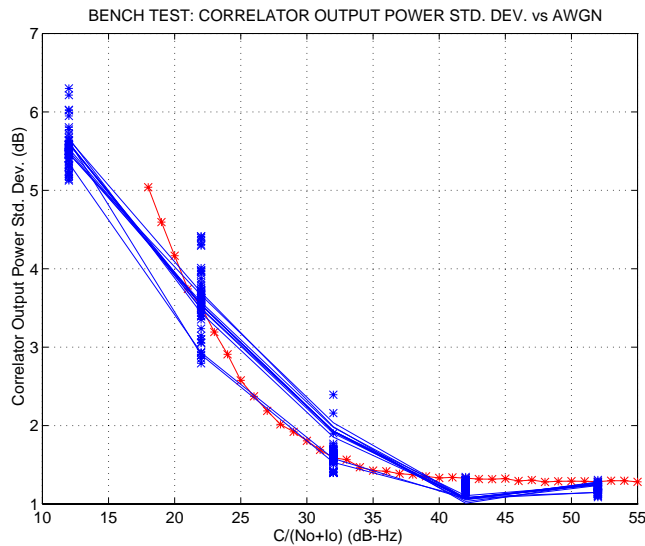


Figure 14: Correlator Output Power Variance vs C/N_0 , AWGN, for Bench Test and Simulation.

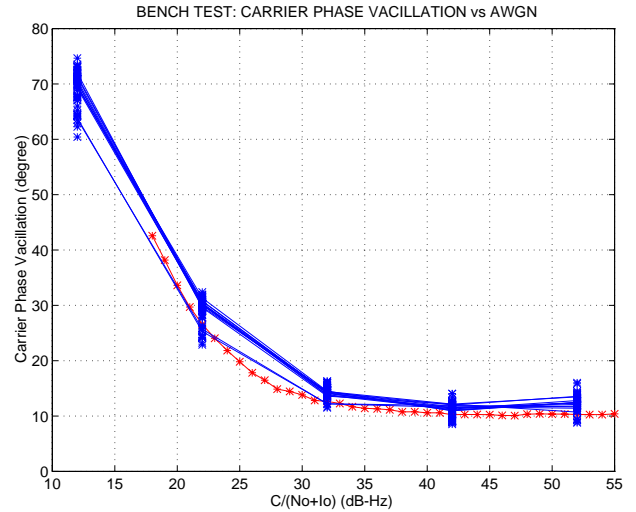


Figure 15: Carrier Phase Vacillation vs C/N_0 , AWGN, for Bench Test and Simulation.

4. INTERFERENCE MITIGATION VIA USE OF PSEUDOLITES

Airport pseudolites (APLs), while producing pulsed interference, also help to mitigate interference by providing a strong navigation signal impervious to many forms of interference. Figures 16 and 17 below show results of a covariance analysis for no APL - differential GPS only, and for augmentation with 2 intrack APLs providing differential carrier phase measurements.

APLs are pulsed, each with a 10% duty cycle. Vertical position error, $2\sigma_v$, is shown against $C_{zenith}/(N_0+I_0)$ over a 24 hour period. A 24-satellite almanac is used for a receiver located at San Francisco International airport.

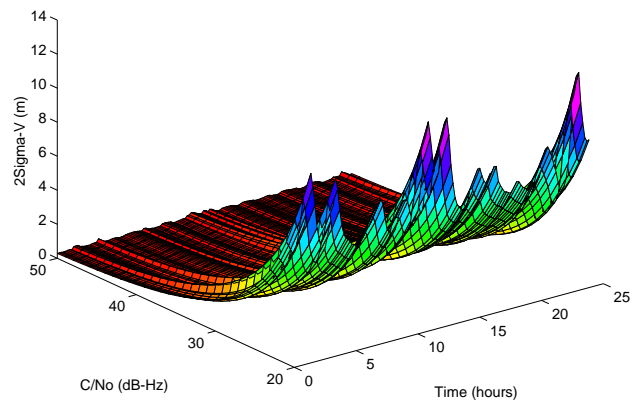


Figure 16: $2\sigma_v$ vs. $C_{zenith}/(N_0+I_0)$ over time for DGPS

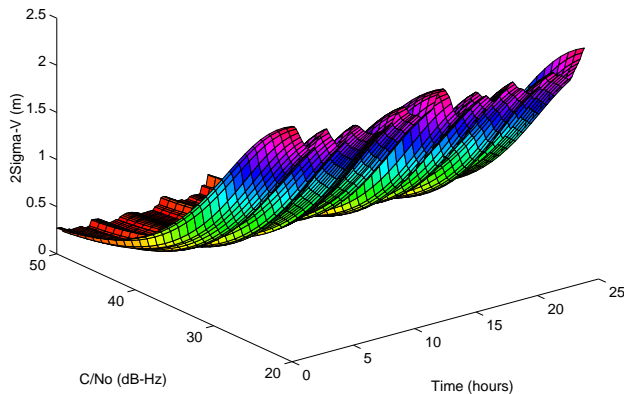


Figure 17: $2\sigma_v$ vs. $C_{zenith}/(N_o+I_o)$ over time for 2 APLs

From the figures, it can be seen that the 2-APL solution provides a more robust and reliable solution than DGPS, with a worst case error of 2.5m, compared to 12.8m for DGPS, corresponding to a high interference environment with $C/N_o = 20$ dB-Hz.

5. CONCLUSIONS

In conclusion we have examined four observable receiver parameters as candidate decision statistic for integrity monitoring, and have demonstrated the reliability and robustness of these parameters. Correlator output power shows best consistent performance under varying levels as well as types of interference. Similar conclusions apply to carrier phase vacillation and standard deviation of correlator output power, without the marked sensitivity to severe coherent CW interference. AGC gain, while showing consistent performance within either pulsed or non-pulsed interference, produces markedly higher decision threshold values for pulsed interference as a result of its pulse suppression role. AGC gain also shows little sensitivity to signal attenuation. While this result indicates its unsuitability for use as the sole decision statistic, it also shows AGC gain to be a beneficial resource for interference type discrimination.

In operation integrity monitoring should be achieved using a combination of all four test statistic. We recommend that correlator output power be the primary indicator, with $COP\sigma$, and carrier phase vacillation as backup indicators. AGC gain may be used to discriminate between types of interference.

Airports pseudolites have been shown to provide for robustness against interference and weak GPS signals.

ACKNOWLEDGMENTS

The authors gratefully acknowledge the support and assistance of the FAA-Stanford WAAS research grant.

REFERENCES

- [1] C. Shively, Y. Lee, "A Position-Domain Ground-Based Integrity Method for LAAS", Institute of Navigation, GPS Technical Meeting, September 1996.
- [2] B. Parkinson, J. Spilker, P. Axelrad, P. Enge, *Global Positioning System: Theory and Applications*, AIAA Washington DC, 1996
- [3] T. Walter, P. Enge, "Weighted RAIM for Precision Approach", Institute of Navigation, GPS Technical Meeting, September 1995.
- [4] Cahn, C. R. et al, "Software Implementation of a PRN Spread Spectrum Receiver to Accommodate Dynamics", IEEE Trans. on Communications, Vol. COM-25, No. 8, August 1977
- [5] M. Johnson, R. Erlandson, "GNSS Receiver Interference: Susceptibility and Civil Aviation Impact", Institute of Navigation, GPS Technical Meeting, September 1995.
- [6] C. Hegarty, "Analytical Derivation of Maximum Tolerable In-Band Interference levels for Aviation Applications of GNSS", Institute of Navigation, GPS Technical Meeting, September 1996.
- [7] B. Parkinson, P. Axelrad, "Autonomous GPS Integrity Monitoring Using the Pseudorange Residual", *Navigation: Journal of The Institute of Navigation*, Vol. 35, No. 2, Summer 1988.
- [8] F. Amoroso, "Performance of the adaptive A/D converter in combined CW and Gaussian interference", IEEE Transactions on Communications, Vol. COM-34, No. 3, March 1986.